Corrosion protection method and performance for prestressing strands

In-Seok Yoon [1], Thomas H.-K. Kang [2], Hyeongyeop Shin [2]

[1] Construction Info. Eng., Induk University, Republic of Korea

[2] Architecture and Architectural Eng., Seoul National University, Republic of Korea

In this study, the performance of corrosion protection systems used in post-tensioning construction fields is discussed. First, a literature review of prior research on stress corrosion is conducted, followed by in-depth review of corrosion protection methods applied in the field of post-tensioning construction, and finally performance of single strand specimens having bonded (grouted) strand, unbonded (greased) strand, and greased sheathed strand (GSS) with and without grouting is investigated using test results of electrochemical and weight loss measurement conducted in accordance with modifications based on PTI M55.1-12 specification. Corrosion was activated by: chloride ion (Cl-), and chloride ion and dissolved oxygen (Cl- + DO). The investigation indicated that all specimens using HDPE (high-density polyethylene) sheath showed excellent corrosion protection performance.

Key words: Corrosion protective system, chloride, dissolved oxygen, HDPE, grease, cement grout

1   Introduction

Corrosion-related failures of prestressing strands were reported in the late 1990's in the USA (Lau, 2016), and strand failure was examined in a concrete viaduct in the Republic of Korea (Son, 2016). Understanding of strand corrosion is important for the development of durable post-tensioned (PT) concrete structures.

This study is devoted to an in-depth review of stress corrosion and current corrosion protection methods for multi PT strands for design application. To examine performance of corrosion protection systems widely used in the multi-strand PT construction fields, the electrochemical method was chosen.

2   Technical background

2.1   *Previous researches on stress corrosion*

Typical causes of prestressing strand corrosion and concern have been attributed to poor grouting, development of bleed water and subsequent re-absorption or evaporation (Powers, 1999; Hansen, 2007; Trejo et al., 2009). In addition, corrosion failure of post-tensioning strands in Europe has been attributed to grout segregation (Bertolini and Carsana, 2011). Main causes of premature prestressing strand corrosion have been attributed to chloride or sulfate ions, micro-cracks, oxygen, voids in cement grout filled ducts, and humidity (Figg Bridge Engineers, 2010).

When cement grout is exposed to salt water or CO_2 gas, corrosion can be initiated by chloride ions penetration or carbonation, as shown in Figure 1. After corrosion initiation, the rate of corrosion is governed by various factors such as oxygen inflow, water content, electrical resistance, and pH of cement grout (FHWA, 2014). It is reported that gypsum grout, with low pH and high chloride or sulphate content, caused accelerated corrosion of strands (O'Reilly et al., 2012). Reis (2007) examined elemental composition of corrosion products on surfaces of strands by means of EDX (Energy-Dispersive X-ray microanalysis), however, there was no evidence of chloride or significant amounts of sulphate present on any surfaces of samples.

The strand at ions and galvanic interaction with the metal ducts and anchorages increase macrocell corrosion.
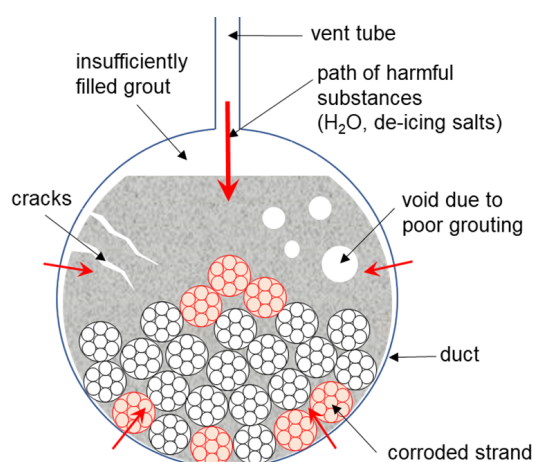

Figure 1: Causes of corrosion in PT duct

Prestressed concrete members have three life cycle stages: (1) crack initiation stage, (2) slow crack propagation stage, and (3) fast crack propagation stage, which induces a rapid brittle failure of prestressing strand by stress corrosion cracking (Brown, 1968). Stress corrosion cracking is due to hydrogen embrittlement. The higher the strength of the prestressing strand the more vulnerable it is to hydrogen embrittlement and potential failure (Fricker and Vogel, 2007). The higher degree of corrosion coupled with higher levels of prestress leads to higher losses of prestress. This loss may need to be accounted for as an additional loss at the design stage (O'Flaherty et al., 2017).

Stress corrosion can be electrochemically divided into two types: anodic and cathodic. The anodic type, which occurs at the site of the anode in a corrosive situation, exists in many different types of environment. Each metal requires a specific active agent which produces the stress crack. The cathodic type takes place at the cathode and is generally associated with hydrogen embrittlement because of the release of hydrogen at the cathodic site. Hydrogen is generated at the cathode as a result of loss of metal at the anodic site.

Stress corrosion cracking is the growth of crack formation in a corrosive environment. The initiation and propagation of stress corrosion cracking is a very complex degradation process governed by many parameters. These parameters can be classified as microstructural, mechanical and environmental.

Microstructural factors include: grain boundary chemistry and segregation; thermal treatment which can cause intragranular and intergranular metallic carbide distribution; and grain size along with cold work or plastic deformation which determines yield strength. These factors are depicted Ⓐ in Figure 2.

Mechanical factors include: applied and residual stresses. These stresses can be described as stress intensity "K" (optionally, strain and strain rate).

Environmental factors include: temperature T; activity of [H^+]; solution or water chemistry; and inhibitors or pollutants in solution. These last two are shown as [x] in Figure 3. In addition, environmental factors include: electrode and corrosion potentials E and E_o, and partial pressure of hydrogen which reflects on potential (Aly and Neto, 2014).
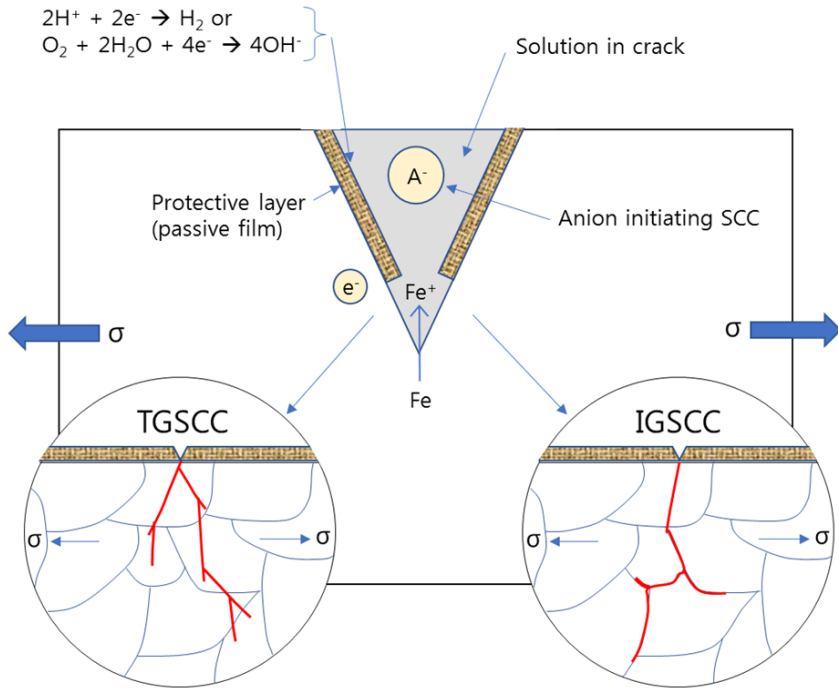
2H$^+$ + 2e$^-$ → H$_2$ or
O$_2$ + 2H$_2$O + 4e$^-$ → 4OH$^-$

Solution in crack

Protective layer
(passive film)

A$^-$

Anion initiating SCC

e$^-$ Fe$^+$

σ σ

Fe

TGSCC

IGSCC

σ σ σ σ

Figure 2: Mechanism of stress corrosion cracking [Woodtli and Kieselbach, 2000]

Depth of SCC
penetration

pH

Environmental
species

Electrode
potential

Corrosion
potential

Temperature

$$x = A\,[H^+]^n\,[x]^p\,K^m\,e^{\frac{E-E_o}{b}}\,e^{\frac{Q}{RT}}\,t^q$$

Alloy composition
Alloy structure

Stress intensity
(optically instead of
K, ε or ε can be used)

Time

Figure 3: General relationship for stress corrosion cracking process depending on many parameters
with adjusted constants of b, m, n, R, p, and q, thermal energy Q, and universal gas constant of R
[Staehle, 2001]

Stress corrosion cracking can be examined and categorized by crack path: trans-granular stress corrosion cracking (TGSCC) and inter-granular stress corrosion cracking (IGSCC), as shown in Figure 2. Depending on the environment and condition of the metal, stress corrosion cracking progresses along the transgranular or intergranular. For carbon steel, TGSCC can happen in a corrosive liquid environment such as: Ammonia, H_2S solution, CO-CO_2-H_2O, cyan solution, and so on. Whereas, IGSCC can occur under a corrosive medium combination of Nitrate solution or NaOH.

Tendon failure is usually induced by atomic hydrogen that penetrates the metal lattice. Conditions required for cracking are: sensitive material, tensile stress and an environment that produces atomic hydrogen on the steel surface. The atomic hydrogen on the steel surface may induce initiation and propagation of cracks starting from the metal surface, especially in the presence of notches or localized corrosion attack. Even in the absence of flaws on the surface, atomic hydrogen may penetrate the steel lattice, accumulate in areas of defects, and lead to brittle failure (Bertolini et al., 2013).

Stress corrosion cracking is also characterised by the evolution of pitting corrosion attacks that result in the development of both micro-cracking and micro-voids in the steel bulk (Vu et al., 2009). Evolution requires the presence of a stress - either residual, applied, or in combination, a specific corrodent and a susceptible strand (Sedriks, 1996). It can lead to unexpected sudden failure of the strand when subjected to a tensile stress, in particular, at elevated temperatures. A reduction in the elastic modulus and the elastic limit, which reach 25% and 15%, respectively, can be expected due to steel micro-cracking (Vu et al., 2009).

Stress corrosion cracking is also highly chemically specific in that certain alloys are only likely to undergo cracking when exposed to explicit chemical environments. The chemical environment that causes stress corrosion cracking can often be one which is only mildly corrosive to the metal. Metal parts with severe stress corrosion cracking can appear bright and shiny, while being filled with microscopic cracks. This factor makes it common for stress corrosion cracking to go undetected prior to failure. The specific environment is of crucial importance. Only very low concentrations of certain highly active chemicals can lead to catastrophic cracking, often leading to devastating and unexpected failure (NPL, 1982).

2.2 *Corrosion protection methods for post-tensioning multi-strand tendon*

Multi-strand tendon consists of multiple bare strands in a post-tensioning duct. The strands are pulled after pouring concrete through a pre-installed duct. After the strands are placed, the interior of the duct is filled with cement grout or flexible filler materials to prevent corrosion of the strands.

Depending on the filler materials and strands, corrosion protection methods for post-tensioning tendon can be classified into: (i) grouted (bonded) tendon; (ii) unbonded tendon with flexible fillers; and (iii) extruded greased sheathed-strand (GSS) tendon with grouting as shown in Figure 4. The grouted tendon consists of multiple bare-strands with cement grout filling the inside of the duct. Since cement grout is injected into the duct and hardened after tensioning of strands, the strands and cement grout are bonded mechanically. The bonded tendon is the most widely used method for corrosion protection, since cement grout is relatively cheap when compared to other filler materials. The unbonded tendon is composed of multiple bare-strands with flexible fillers such as grease or wax filling into the duct after post tensioning. Likewise, the strands are not bonded to the surrounding duct and concrete. In short, the tendon is mechanically unbonded, which means that strain compatibility is not established between the tendon and surrounding concrete. The extruded greased sheathed-strand (GSS) tendon consists of multiple GSSs and cement grout. Each GSS for this study is comprised of: a 7-wire strand, PT coating (i.e., grease) and high-density polyethylene (HDPE) sheath. The inside of the duct is filled with cement grout, but the tendon is mechanically not bonded to surrounding concrete.

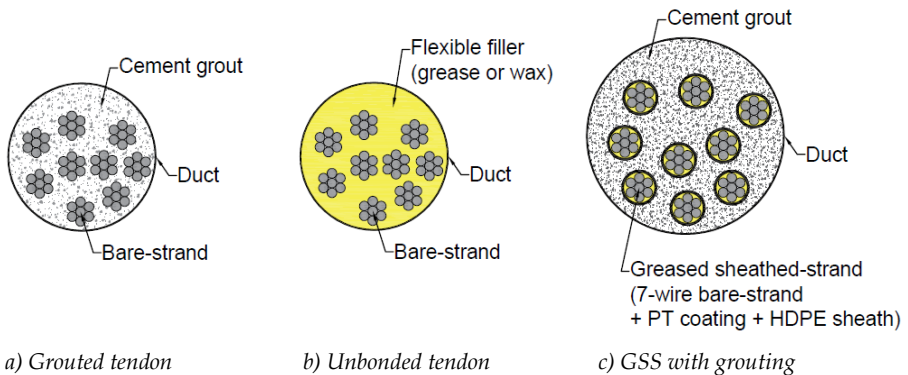a) Grouted tendon   b) Unbonded tendon   c) GSS with grouting

Figure 4: Typical section compositions of each post-tensioning method

The grouted tendon is the most economical system among the three systems in Figure 4, since cement grout used to fill the duct is relatively inexpensive. Whereas, the conventional unbonded tendon is considered uneconomical in terms of material cost, since flexible fillers (wax or grease) are relatively expensive. In the case of the GSS tendon, total material cost is higher than the grouted tendon but lower than the unbonded tendon utilizing flexible fillers.

In construction of post-tensioned structures, both bonded tendon and unbonded tendon with flexible fillers are constructed in the following sequence: (i) concrete curing and strand installation; (ii) tensioning of strands, and (iii) injection of cement grout or flexible fillers. Because tensioning of strands is conducted after curing of the outside concrete, the construction period is relatively long. Given the strands are exposed to the outside air before injection of cement grout/flexible fillers, there is the possibility of strand corrosion during the construction. However, these two systems have an advantage over the GSS tendon in that they have relatively small duct size. Current code and specifications such as AASHTO (2017), FHWA (2013), and PTI (2012) require 2.0 to 2.5 in terms of duct/tendon area ratio.

In the case of GSS tendon, strand installation and cement grout injection/curing can be done during curing of the outside concrete resulting in an overall shorter construction period. The down side is that the use of GSS increases the cross-sectional area of the strands, resulting in a relatively larger required duct size. In addition, threading of GSSs is more difficult since sheathing damage can occur during the installation.

In terms of structural performance, bonded tendon and unbonded tendon with flexible fillers experience large prestress loss due to friction. Because bare-strands are in contact with each other, friction between the strands and duct surface exists during tensioning. In addition, strands can become twisted and tangled during individual strand installation. There is also the possibility that some strands may become damaged due to compression between the tangled strands. Whereas, GSSs have independent paths provided by HDPE sheathing. Even though entanglement between strands exists, there is no friction between strands or compression failure. Given independent pathways, GSS tendon has very low associated friction coefficients. In PTI/ASBI (2012), recommended values for curvature and wobble friction coefficients are 0.15 ~ 0.25/rad and 0.000164 ~ 0.000984/m, respectively for GSS tendon and 0.01 ~ 0.05/rad and 0.000164 ~ 0.000984/m, respectively for conventional tendon using corrugated metal duct.

With regard to maintenance, old strands of bonded tendon cannot be replaced by new strands due to the hardened cement grout within the duct. In addition, it is not possible to directly measure prestress force of the tendon using lift-off test while in service. In the case of unbonded bare-strand tendon, strand replacement is possible. But all of the strands should be de-tensioned, replaced and re-tensioned. In other words, it is not possible to replace only one strand without detensioning/replacing other strands in the tendon, since bare-strands are engaged with each other. For similar reasons, tensile force measurement for in service strands through lift-off test can be made for the entire tendon, but lift-off test of individual strand is not possible. On the other hand, replacement and tensile force measurement of individual strands are possible in the grouted GSS tendon, due to independent path of the strand provided by HDPE sheathing.

In terms of durability (i.e., corrosion protection), the bonded tendon has a layer of cement grout that protects strands from penetration of harmful substances such as water or chloride ions. If water and/or chloride ions penetrate into cement grout, strands may be vulnerable to corrosion. The main causes of harmful substance penetration route are as follows: (i) insufficient filling of the duct with cement grout; (ii) cracks due to drying shrinkage; and (iii) voids generated by bleeding (Figure 1). The unbonded tendon also has a single corrosion protection layer provided by flexible fillers. As is for the bonded tendon, the duct may not be sufficiently filled with flexible fillers. Also due to the material characteristics of flexible fillers – gel like state, the fillers may leak out of the duct at connection and near anchorage, especially in vertical installations, resulting in voids (Figure 5a). In the case of grouted GSS tendon, a 7-wire strand is protected from corrosion by cement grout, HDPE sheath and PT coating (grease). However, HDPE sheath damage may occur during the installation of GSSs and create infiltration pathways for harmful substances (Figure 5b).

Since prestressing strands are inserted into an empty duct, the strands are not uniformly distributed and often eccentrically arranged resulting in strands placed in direct contact with the conventional corrugated metal duct surface and not encased or properly protected from corrosion-inducing substances by cement grout or flexible fillers. This may not be a problem for GSS tendon, as the extruded HDPE-coated strands are still resistant to corrosion (Figure 6).
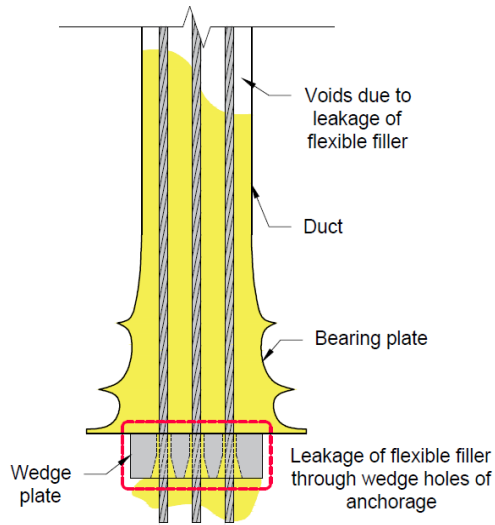
a) Leakage of flexible filler in vertically installed unbonded bare-strand tendon
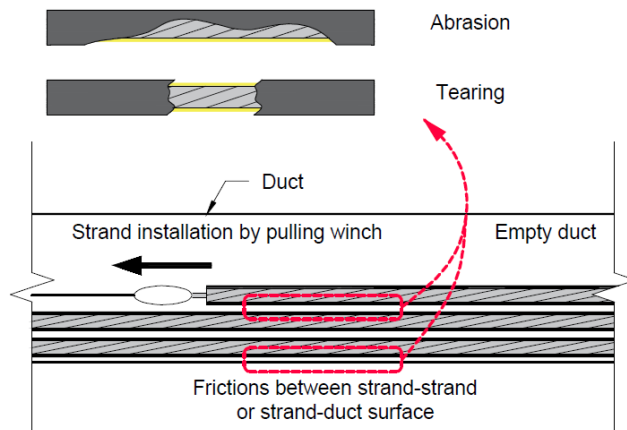
b) HDPE sheath damage during installation in GSS tendon
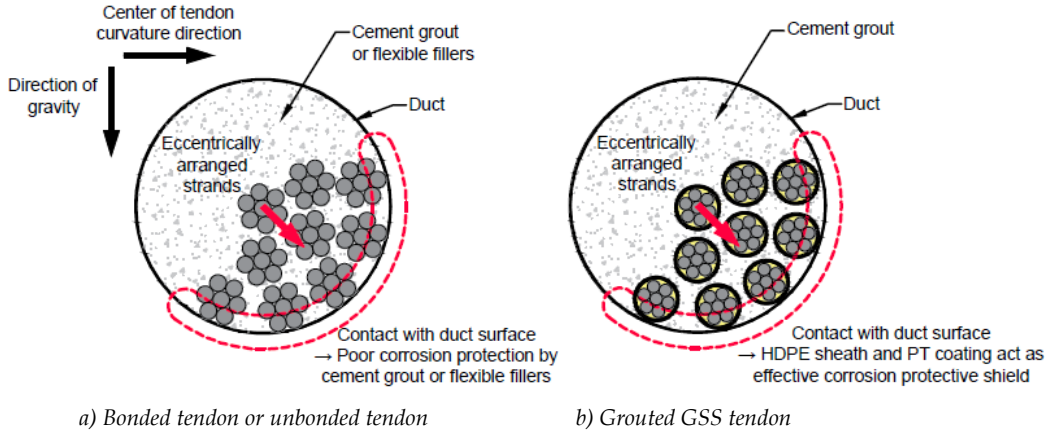
Figure 5: Adverse factors on corrosion resistance

a) Bonded tendon or unbonded tendon   *b) Grouted GSS tendon*

Figure 6: Corrosion risk due to eccentrically arranged strands

3   Investigation of corrosion tests

3.1   *Specimens*

The selected specimens from the corrosion tests of the authors (Yoon et al., 2019) are shown in Figure 7. For all specimens, a 7-wire strand with a nominal diameter of 15.7 mm was used, and the length was 120 mm. Figure 7a shows a 7-wire bare-strand (PS-0) where corrosion protection is not applied. Figure 7b shows a strand protected by oil grease (PS-G) applied throughout the bare-strand exterior surface. Figure 7c shows a cement grout-protected specimen (PS-C) which was prepared to evaluate the corrosion resistance of bonded tendon. The thickness of the cement grout coating chosen was 7.2 mm. Figure 7d
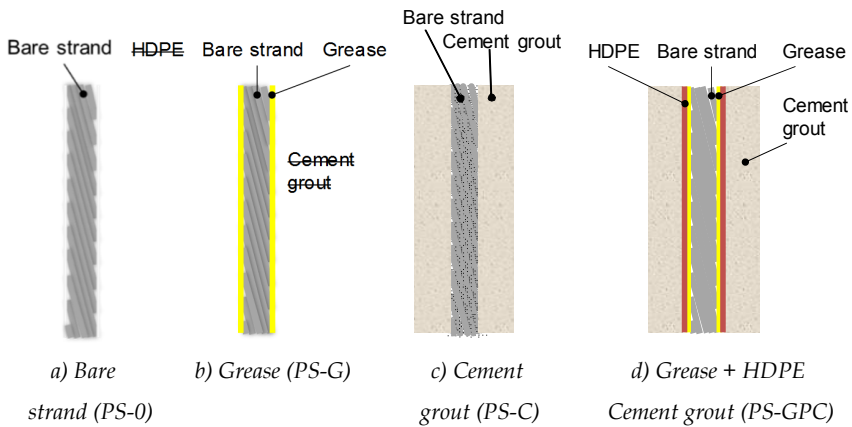

a) Bare strand (PS-0)   *b) Grease (PS-G)*   *c) Cement grout (PS-C)*   *d) Grease + HDPE Cement grout (PS-GPC)*

Figure 7: Experimental variation for corrosion-protection system in specimen

shows a GSS that is also protected by cement grout (PS-GPC). Here, the thicknesses of grease, plastic sheath and cement grout were 0.4 mm, 1.0 mm, and 5.8 mm, respectively.

For all the specimens with the exception of specimen PS-0 (bare-strand), both ends of the duct were sealed with epoxy so that the 7-wire strands would not be exposed to air or solution in the corrosion test cell.

3.2 *Corrosion cell*

To evaluate the corrosion resistance of each post-tensioning method, the experiment apparatus designed is as shown in Figure 8. The apparatus differs slightly from the accelerated corrosion test (ACT) method specified in the Appendix B of PTI (2012). The chloride ion (Cl⁻) concentration made by dissolving sodium chloride (NaCl) in distilled water for the corrosion cell was 5%.

Two series of experiments were investigated with this type of corrosion activation: 1) chloride ion only; and 2) both chloride ion and dissolved oxygen. In order to evaluate corrosion by chloride ion and dissolved oxygen, the concentration of dissolved oxygen was 21 ppm when measured by dissolved oxygen meter (DO meter). Consequently, a total of sixteen specimens were investigated: 1) two specimens per type with chloride ion only and 2) two specimens per type with both chloride ion and dissolved oxygen.

Strands were polished with sandpaper and then cleaned up with acetone. Cement grouting was cured for 28 days and the formulation was based on the common post-tensioning grouting used in the Republic of Korea.

3.3 *Electro-chemical measurement*

Corrosion of prestressing strand specimens protected by each protection method was electrochemically estimated based on the polarization resistance method. Polarization resistance (R_p) is defined as the ratio of the applied voltage (ΔE) (shift in potential from E_{corr}) to current step (ΔI), when the metal is slightly polarized (about 20 ~ 50 mV) from its free corrosion potential (E_{corr}) (Andrade and Alsonso, 2004). In this study, the potential static method was used for corrosion measurement based on the polarization resistance method. A graphite rod was used as a counter electrode, and a saturated calomel electrode was used as a reference electrode. The working electrode was a prestressing strand specimen. The electrodes were connected to an electrostatic potential device, and the potential of the working electrode was measured as current was applied.
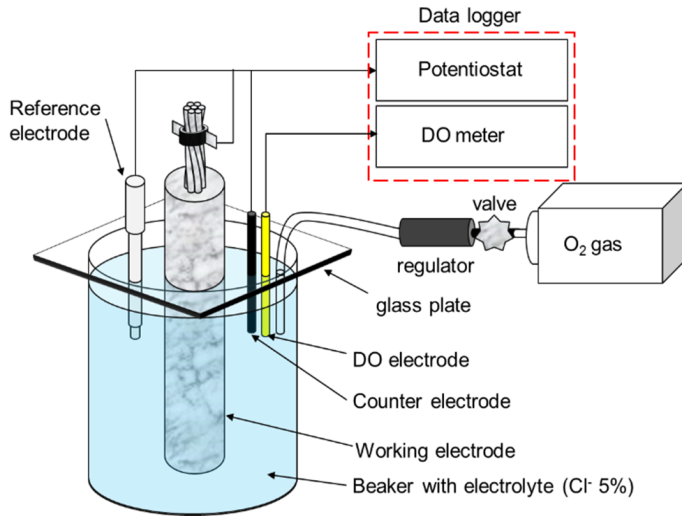
a) Accelerated corrosion test apparatus
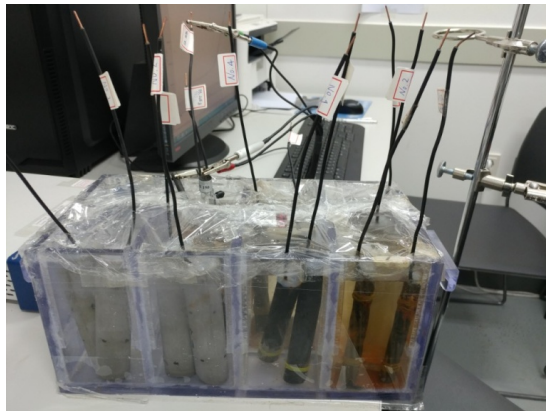
b) During corrosion test

Figure 8 : Corrosion cell set-up

The linearity of current-potential is known to be in the range of 20 to 30 mV for reinforcing steel. When subject to a high corrosion rate, it is known to be linear in the range of 100 mV (Polder et al., 1993). Due to a lack of research on the linear range of prestressing steel, a current corresponding to –10 ~ +10 mV with respect to open-circuit potential (E_{oc}) was applied. The prestressing strand specimens were immersed in the corrosion solution for 60 days, and corrosion current density was measured every 15 days.

3.4 Measurement of weight loss

To evaluate the degree of corrosion, weight loss of the prestressing strand due to corrosion was measured. Strand weight was measured before and after the corrosion test. A precision balance with 0.1 mg of sensitivity was used to provide accurate weight measurements. At the end of the corrosion test, the prestressing strand specimen was taken and impurities along with corrosion products removed. The prestressing strand was immersed in a cleaning solution and the corrosion product was removed using a resin brush. The cleaning solution was mixed with 20 g of antimony trioxide (Sb_2O_3) and 50 g of stannous chloride ($SnCl_2$) in 1 L of hydrochloric acid (HCl) solution. The cleaning procedure followed ASTM G1 (ASTM, 2017).

4   Discussion

4.1 Corrosion due to chloride solution

The corrosion current density of the specimens over time was obtained from the accelerated corrosion test by chloride (Cl^-) solution (Figure 9). The PS-0 specimens, not having any corrosion protection layer, had very high corrosion current densities. Corrosion current densities measured were higher than 80 $\mu A/cm^2$ in 15 days. Specimens with application of corrosion protection methods had significantly lower corrosion rates.

Specimens coated with grease "PS-G" and cement grout "PS-C" for corrosion protection exhibited similar levels of corrosion current densities. However, the time-dependent response was different. The PS-G specimens showed a tendency of increasing corrosion current density over time indicating that the grease coating of the specimen immersed in the chloride solution had been damaged. In other words, portions of the grease coating were washed out in the solution. The grease coating effectively protected the strand from chloride ion intrusion at the initial stage of experiment, but gradually allowed penetration of chloride ion due to the loss. Because the persistency of ion penetration resistivity of the grease coating may vary depending on the concentration of ion along with the type and thickness of the grease coating, further study is recommended.

The PS-C specimens showed a decreasing trend of corrosion current density over time. The specimens had fine cracks on the surface of hardened cement grout. Because fine cracks often occur in construction, corrosion test was carried out without any repair to reflect the actual field conditions. For corrosion test, the corrosion reaction may be affected by the

surface condition. Rapid penetration of chloride ions through the microcracks on the cement grout surface led to a rapid corrosion at the initial stage of testing. However, over time, the corrosion product layer on the surface of prestressing steel delayed penetration of chloride ions, and the measured corrosion current density reduced. For bonded tendons, improved corrosion resistivity can be achieved if high quality control is maintained during construction to minimize fine cracks.

The PS-GPC specimens, as anticipated, exhibited the lowest corrosion current density and the best corrosion protection performance among all the specimens tested in this study. The experimental results confirm the superior corrosion resistance of the GSS tendon system.

4.2 *Corrosion protective performance*

Average corrosion current density for each specimen is shown in Figure 9. The average corrosion current density was high in the order of PS-0, PS-G, PS-C, and PS-GPC. The PS-G specimens with grease coating and the PS-C specimens with cement grout had the same level of corrosion rate in chloride ion (Cl-) solution corrosion test. However, in the corrosion test with chloride ion and dissolved oxygen (Cl- + DO) solution, the PS-G specimens showed a higher average corrosion current density. Since the thickness of PT
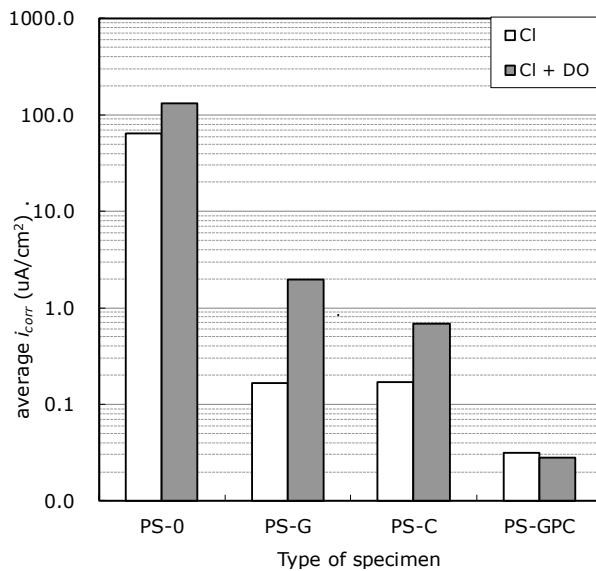

Figure 9: Average corrosion current density

coating (grease) and cement grout applied to each specimen was different, it is difficult to directly compare their corrosion resistance performance. Unlike the current test condition of directly immersed specimens in the corrosive solution, there will be little loss of grease on the strand surface due to the presence of post-tensioning duct in actual construction. Therefore, with the same thickness and corrosive environment, post-tensioning method using grease is expected to be similar to that with cement grout. The PS-GPC specimens showed the lowest corrosion rate.

4.3   *Weight loss of strand*

Figure 10 shows weight loss of the prestressing strand due to corrosion. The PS-0 specimens, which had no applied corrosion protection, had very severe weight loss. The weight loss due to corrosion by chloride ion and dissolved oxygen was twice the weight loss by chloride ion solution and lied in close agreement with the results of corrosion current density.

Weight loss due to corrosion had increased significantly when the specimens were exposed to chloride ion and dissolved oxygen in order to replicate a complex corrosive environment. In particularly, the PS-G specimen, which was protected by only grease coating, experienced about 20 times the difference in weight loss due to chloride ion
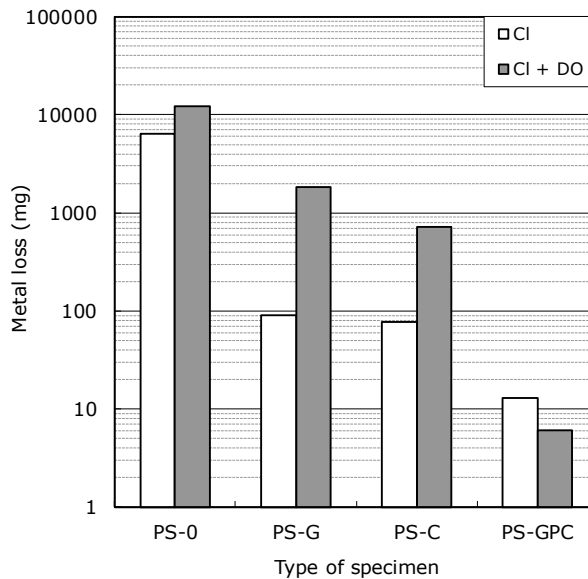

Figure 10: Amount of metal loss of strand due to corrosion

solution alone. This difference is attributed to damage to the grease coating caused physically by gaseous oxygen bubbles.

Weight loss of the PS-GPC specimens with HDPE sheath showed a tendency similar to measured corrosion current densities. Here, the HDPE sheath served as an effective barrier to block the inflow of chloride ion or oxygen.

It is concluded that the corrosion protection performance of each corrosion protection method was consistent with the tendency found in the corrosion current density measurement. The current experimental study is of value, as it is the first with respect to scientific verification of the corrosion protection performance.

5   Conclusions

The corrosion protection systems for the widely used multi-strand post-tensioning methods (bonded tendon, unbonded tendon, and grouted GSS tendon) were compared and discussed. The grouted GSS system exhibited the best test result, scientifically demonstrating superior corrosion protection performance.

Results of this study should be used as a basis for further research for assessment of corrosion protection performance of prestressed and post-tensioned concrete structures. In addition, data derived can be used as a basis for selecting post-tensioning method type for a wide array of concrete structures: buildings, reservoirs/tanks, bridges, nuclear containment structures and shelters among others that have varying degrees of durability requirement and environmental conditions.

54

Literature

AASHTO (2017). AASHTO LRFD Bridge Design Specifications, 8th Ed. American Association of State Highway Transportation Officials, Washington D.C.

Aly, O. F., and Neto, M. M. (2014). Stress Corrosion Cracking, *Intech.*

Andrade, C., and Alonso, C. (2004). Test Methods for On-Site Corrosion Rate Measurement of Steel Reinforcement in Concrete by Means of the Polarization Resistance Method. *Materials and Structures*, 37(9) : 623-643.

ASTM (2017). ASTM G1-03. Standard Practice for Preparing, Cleaning, and Evaluating Corrosion Test Specimens (Reapproved 2017). ASTM International, West Conshohocken.

Bertolini, L., and Carsana, M. (2011). *High pH Corrosion of Prestressing Steel in Segregated Grout. Modeling of Corroding Concrete Structures*. RILEM Book Series, 5. RILEM.

Bertolini, L., Elsener, B. Pedeferri, P., Redaelli, E., and Polder, R. (2013). *Corrosion of Steel in Concrete*, 2nd Edition. Wiley-VCH, 155-170.

Brown, B. F. (1968). The Application of Fracture Mechanics to Stress Corrosion Cracking, *Metallurgical Review*. 13(1) : 171-183.

Lau, K. (2016). Corrosion of Post-Tensioned Tendons with Deficient Grout. Final Report, Project BDV29-977-04, FDOT Research Center, Miami.

FHWA (2013). Post-Tensioning Installation and Grouting Manual. U.S. Dept. of Transportation Federal Highway Administration, McLean.

FHWA (2014). Post-Tensioning Tendon Grout Chloride Thresholds. An FHWA Special Study, U.S. Dept. of Transportation Federal Highway Administration, McLean.

Figg Bridge Engineers, Inc. (2010). I-295. Verina-Enon Bridge Tendon Replacement for the Virginia. Virginia Department of Transportation, Exton.

Fricker, S., and Vogel, T. (2007). Site Installation and Testing of a Continuous Acoustic Monitoring. *Construction and Building Materials*, 21(3) : 501-510.

Hansen, B., (2007). Forensic Engineering: Tendon Failure Raises Questions about Grout in Post-Tensioned Bridges. *Civil Engineering News*, 77(11) : 17-18.

NPL (1982). Guides to Good Practice in Corrosion Control: Stress Corrosion Cracking. The National Physical Laboratory.

O'Flaherty, F., Elomari I.R., and Lambert, P. (2017). Corrosion Induced Losses in Prestressed Tendon. 37th Cement Concrete Science Conference, London, 111-115.

O'Reilly, M., Darwin, D., and Browning, J. (2012). Corrosion Performance of Prestressing Strands in Contact with Dissimilar Grouts. The University of Kansas Center for Research, Inc., Lawrence, 111-115.

Powers, R. G. (1999). Corrosion Evaluation of Post-Tensioned Tendons on the Niles Channel Bridge. Florida Department of Transportation, Gainesville.

Polder, R., Tondi, A., and Cigna, R. (1993). Concrete Resistivity and Corrosion Rate of Reinforcement. TNO Report 93-BT-r0170, TNO, Netherlands.

PTI (2012). PTI M55.1-12. Specification for Grouting of Post-Tensioned Structure. Post-Tensioning Institute, Farmington Hills.

PTI/ASBI (2012), PTI/ASBI M50.3-12. Guide Specification for Grouted Post-Tensioning. Post-Tensioning Institute, Farmington Hills.

Reis, R. A. (2007). Corrosion Evaluation and Tensile Results of Selected Post-Tensioning Strands at the SFOBB Skyway Seismic Replacement Project Phase III Report. Materials Engineering and Testing Services, Office of Testing and Technology Services Corrosion Technology Brach, California.

Sedriks, A.J. (1996). *Corrosion of Stainless Steels*. John Wiley & Sons Inc.

Son, D. (2016, June 27). Retrieved October 9, 2018, from https://news.joins.com/article/20226717, (In Korean).

Staehle, R. W. (2001). Bases for Predicting the Earliest Penetrations due to SCC for Alloy 600 on the Secondary Side of PWR Steam Generators. Argonne National Laboratory, 2001, NUREG/CR-6737, ANL-01/20 RWS 151, Argonne.

Trejo, D., Hueste, M. B., Gardoni, P., Pillai, R., Reinschmidt, K., Im, S. B., Kataria, S., Hurlebaus, S., Gamble, M., and Ngo, T. T. (2009). Effect of Voids in Grouted, Post-Tensioned Concrete Bridge Construction: Vol.1-Electrochemical Testing and Reliability Assessment. Report No. 0-4588-1.TTI. College Station.

Vu, N. A., Castel, A., and Francois, R. (2009). Effect of Stress Corrosion Cracking on Stress-Strain Response of Steel Wires Used in Prestressed Concrete Beams. *Corrosion Science*, 51(6) : 1453-1459.

Woodtli, J., and Kieselbach, R. (2000). Damage due to Hydrogen Embrittlement and Stress Corrosion Cracking. *Engineering Failure Analysis*, 7(6) : 427-450.

Yoon, I.-S., Shin, H., and Kang, T. H.-K. (2019). Comparative Study on Performance of Corrosion Protective Systems for Post-Tensioned Concrete Members. *ACI Structural Journal*, 116(3) : 273-284.